N.P. López-Acosta et al. (Eds.)

doi:10.3233/STAL190223

Effect of a DEM in the Estimation of Coherence and Unwrapped Phase InSAR for Landslides Detection

N.A. CORREA-MUÑOZ[a,1], Kevin TANSEY[b] and C.A. MURILLO-FEO[c]
[a] *Full professor at Universidad del Cauca. Ph.D. Student at Faculty of Engineering, Universidad Nacional de Colombia.*
[b] *School of Geography, Geology, and the Environment, Leicester Institute of Space & Earth Observation, University of Leicester, University Road, Leicester, UK.*
[c] *Assistant Professor at Faculty of Engineering, Universidad Nacional de Colombia.*

Abstract. This study applied Synthetic Aperture Radar Interferometry (InSAR) to estimate terrain displacements using four Digital Elevation Models (DEMs). The InSAR workflow was implemented in a region located at southwestern of Colombia. The radar images were processed using ESA's SNAP Toolbox, varying a DEM at the stages back-geocoding, topographic phase removal, and geometric correction. A SLC IW TOPSAR Sentinel-1 A/B radar images were analyzed between October 2014 and November 2016 for S1-A and between October 2016 and March 2017 for S-1B. Four SLC pairs were selected with the smaller perpendicular and temporal baseline for the displacement estimation. The work process implemented was, co-registering, interferogram formation, topographic phase removal, filtering, unwrapping phase and geocoding. The DEMs, SRTM3 (3 arc-second resolution), SRTM1 (1 arc-second resolution), PALSAR-RTC data and interpolation of contour lines at the scale of 1:25K (Topo-map) were used. Exploratory, paired-means and ANOVA analysis allowed to compare the distributions. Likewise, Principal Components Analysis method allowed establishing the relationship between the InSAR parameters - phase, coherence, unwrapped phase, and the displacement -. This analysis was complemented by Logistic Regression methods and Weight of Evidence. As a result of this study, we confirmed an inverse relationship between the unwrapped phase and displacement. Also, the coherence estimated from the four DEMs is highly correlated with the Colombian Geological Service landslide inventory. By WofE analysis, we found that coherence values between 0.43 and 0.67 are significantly related to landslide inventory, as well as displacement values between 0.14 and 0.19 m.

Keywords. Synthetic aperture radar interferometry (InSAR), digital elevation model (DEM), phase, coherence, displacement, binary logistic regression, landslide inventory.

1. Introduction

As landslides are natural hazards causing casualties, infrastructure damage, and economic losses, it is important to map them by using Earth Observation, specifically SAR data. SAR is an active microwave device that records the electromagnetic echo

[1] Corresponding Author, Full professor at Universidad del Cauca, Popayán, Colombia; E-mail: nico@unicauca.edu.co

backscattered from the Earth surface and puts it in a 2D image map, whose dimensions are the sensor–target distance (slant range or Line of Sight direction (LOS)), and the flight direction (azimuth) [1]. A radar signal contains amplitude and phase data. The phase information from SAR images can be exploited using the InSAR approach, a method designed to measure changes in signal phase over time [2].

When two SAR images from slightly different viewing angles are combined (interferometric pair), their phase difference can be used to generate a digital elevation model (DEM) and to monitor terrain changes with a precision of half a wavelength [3].

The phase difference is the basis for the calculation of the interferometric phase. The SAR interferogram is the complex image formed by cross-multiplying the two SAR images, a map of relative changes in the distance between the satellite and the earth surface, expressed as phase differences. Therefore, the phase difference is a function of the relative elevation and the altitude of ambiguity [4].

The simplest way to estimate small motions consists of choosing an image pair with a minimal baseline so that the first term (topographic phase) of the phase difference is smaller than the second. The baseline is the distance between the two satellites (or orbits) so, the smaller the baseline, the lower the topography contribution to the phase [5]. Terrain Observation by Progressive Scans (TOPS) acquisition mode has a wide swath coverage. The Wide Swath Mode (IW) image mode provides swath widths of 250 and 400 km at both ground range and azimuth resolution (5 x 20 m, and 20 x 40 m) [5]

Coherence is a similarity measure between two images that form an interferogram. It compares the complex values of the amplitude and the phase of both images combined into a normalized value, ranging from 0 to 1 [6]. Interferometric coherence gives some indication of the land cover type (i.e., water bodies show low coherence, agricultural fields show a moderate coherence; rocks and artificial targets show high coherence).

The binary logistic regression (BLR) is one of the statistical methods used for assessing landslide susceptibility [7–10]. The application of BLR requires a landslide inventory like the dependent variable and triggering parameters as independent variables. The independent variables can be chosen by principal components analysis (PCA) in order to reduce the multicollinearity [11].

The objective of this study is to select a DEM for estimating the interferogram outputs - phase, coherence, and unwrapping phase – using InSAR workflow for the estimation of terrain displacement. Previous studies have demonstrated the usefulness of this methodology to map and monitor the area affected by ground deformation [12].

2. Methodology

2.1. InSAR processing flow

The InSAR workflow to estimate displacements, on ESA's Sentinel Application Platform (SNAP) [13], is shown in Figure 1. The process where a DEM is required did highlight. DEM is used in the InSAR workflow for the processes of co-registration, correcting SAR geometric distortions, removing the topographic phase, and georeferencing the InSAR products in map coordinates.

- Data was downloaded from Scientific Data Hub-Copernicus from October 2014 till March 2017. Only four pairs of images were selected for this study, with minimal perpendicular baseline [14]. The multi-temporal approach, to get better accuracy in the results, will be treated in another stage of this research.

- In SNAP toolbox: First, orbital state vectors were applied over the master and slave scene using precise-orbit ephemerides. Second, a co-registration onto a common master image and a geocoding to convert coordinates from radar to map geometry. Third, an interferogram is formed without the flat-earth phase and with the estimation of coherence. Then a spatial subset was created to reduce the computational time, followed by removing the phase component due to the variation of the range distance across the SAR image [15]. Next, the phase noise is reduced using an adaptive filter [16]. Phase unwrapping, to estimate displacements, is carried out externally applying the network-flow phase-unwrapping algorithm (SNAPHU) [17]. The InSAR outputs are geocoded in a map coordinate system (WGS84) and exported to GeoTIFF format.
- InSAR products obtained in SNAP and the SIMMA landslide inventory from Colombian Geologic Service were post-processed in SAGA and R software for exploratory statistical analysis. Finally, a logistic regression analysis is run on Arc-SDM (Spatial Data Modeller for ArcView 3.2) package [18].

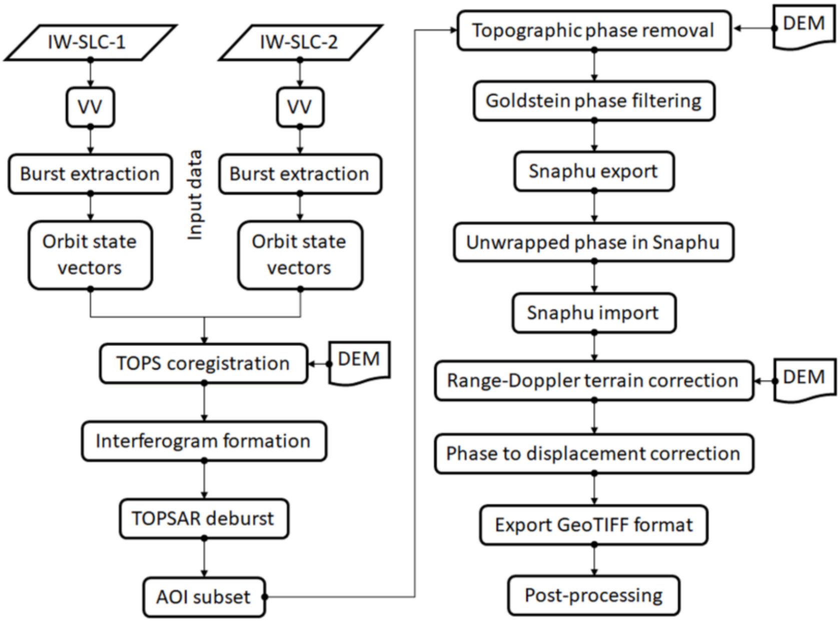

Figure 1. InSAR workflow to displacements estimating in SNAP toolbox.

2.2. Study area

The study area is in western Colombia (2°9'37" north and 76°47'39" west, and 2°28'12" north and 76°27'56" west). Figure 2 shows the areas whose DEM elevation varies between 1004 m and 3698 m above sea level (a.s.l). This region is often affected by landslides. The landslide inventory (LSI) from Colombian Geologic Service (CGS) is displayed as points, containing 107 events: slides (78%), fall (13%), creep (6%), and flow (3%).

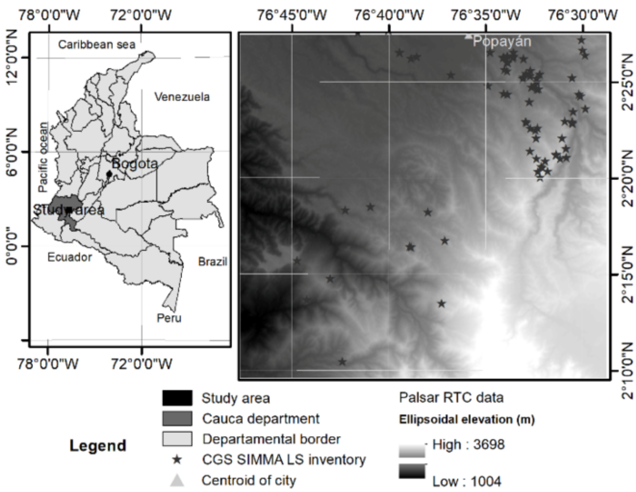

Figure 2. Regional and local localization in the study area.

2.3. DEMs analyzed

We used DEMs SRTM3, SRTM1, Palsar-RTC data, and Topo-map at medium scale (Table1). PALSAR-RTC data correspond to the ALOS-1 radiometric terrain corrected products distributed by ASF-DAAC earth observation service. The Topo map DEM was obtained by 'spline interpolation' method [19], [20] on SAGA software and took as basis contour lines at a scale of 1:25K.

Table 1. Characteristics of medium resolution DEMs used for InSAR processing.

DEM	Source	Resolution (m) or scale
3 arcsec SRTM	Auto download	90
HGT 1 arcsec SRTM	Auto download	30
PALSAR_RTC_hi[2]	ASF's Data Portal	12.5
TOPO map	Colombian Geographic Institute	1:25000

2.4. ESA' Sentinel 1 radar images

A stack of S1 IW TOPSAR[3] images was analyzed (Table 2). The stack has VV polarization and an average incidence angle of 34°. Sentinel-VV polarization was most frequent than VH in the period of analysis.

Table 2. The main feature of ESA's Sentinel 1 stack in the study area.

Platform	Number of available images	Acquisition date	Ascending	Descending
Sentinel-1A-IW	90	20th Oct 2014 / 9th Nov 2016	47	43
Sentinel-1B-IW	34	3rd Oct 2016 / 20th Mar 2017	18	16

[2] Dataset: ASF DAAC 2010, ALOS-1 PALSAR_Radiometric_Terrain_Corrected_high_res; Includes Material © JAXA/METI 2007. 10.5067/Z97HFCNKR6VA.
[3] Copernicus Sentinel data 2014. Retrieved from ASF DAAC 29 April 2017, processed by ESA.

The S1 SAR images selected for deformations estimation are related in Table 3. Interferograms with a perpendicular baseline less than 30 m are easy to unwrap, but they have high sensitivity to phase noise and atmospheric effect [14]. The interferograms with minimal baseline and in the ascending mode were considered in this study.

Table 3. Sentinel-1 SLC SAR images for InSAR processing.

Master SAR image	Slave SAR image	Bp (m)	Bt (days)
S1B-96E4 (Asc) {20161120}	S1B-B4EA (Asc) {20170107]	6.2	48
S1A-E1B8 (Asc) {20160530}	S1A-963E (Asc) {20160611}	2.51	12
S1B-9502 (Asc) {20170107}	S1B-48A7 (Asc) {20170131}	4.65	24
S1B-39AA (Desc) {20161022}	S1B-7CF0 (Desc) {20161115}	5.08	24

3. Results and discussion

3.1. Effect of a DEM on InSAR processing

The interferometric pairs of Table 3 were obtained by varying the DEMs indicated in Table 1. We present the results obtained for the second interferometric phase; they cover the study area with a minimum perpendicular and temporal baseline. The smaller the baseline, the lower the topography contribution to the interferometric phase [5]. First, a random sample of InSAR components of about 1000 points was extracted. The statistical distributions in a plot way for phase, coherence, unwrapped phase, and deformation are shown in Figure 3. A T-Test proved that the interferograms mean it is different at a significance level of 0.001, only for unwrapped phase and displacement. This means that DEM had a significant impact on wrapped differential interferograms [21].

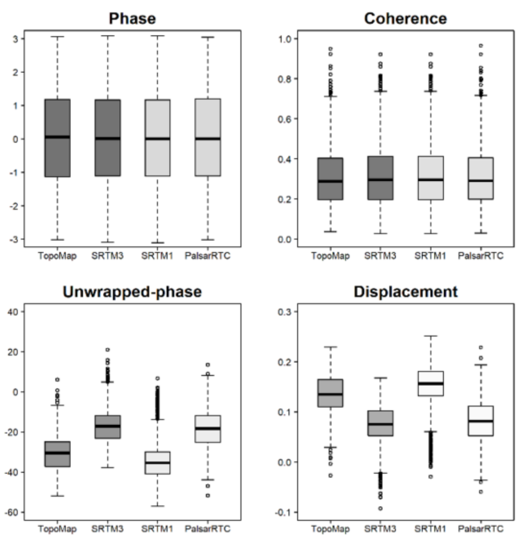

Figure 3. Boxplot chart of InSAR components (random sample).

The extraction of InSAR components for the CGS Landslide Inventory is represented in Figure 4. T-Test showed significant differences in the mean of InSAR coherence between Palsar-RTC data against the other DEMs, due to better spatial resolution [22]. Also, the unwrapped phase showed significant differences at a 0.001 significance level using any DEM. This can be explained due to DEM inaccuracies [21].

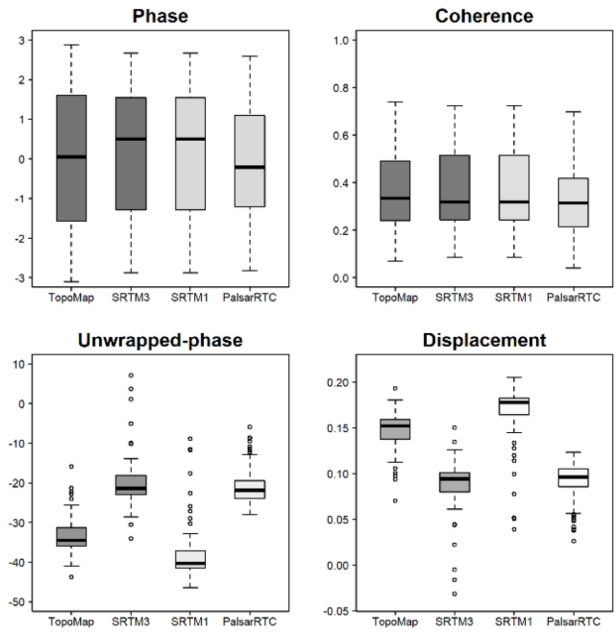

Figure 4. Boxplot chart of InSAR parameters (SIMMA landslide inventory).

3.2. Multivariate analysis

PCA gave us the relationship between InSAR components (Figure 5) [23]. We found a perfect relationship between coherence obtained with SRTM3 and SRTM1 DEM (r=1). In the unwrapped phase, the correlation also was high between the two SRTM DEMs. The InSAR coherence correlation between SRTM3 and SRTM1 DEMs compared with Topo map is high (r=0.74), but low compared with Palsar-RTC data (r=0.24).

3.3. Logistic regression

For the landslide susceptibility modeling, logistic regression was applied with a layer of binary type points, where 0 is stable, and 1 is an unstable event obtained from the CGS landslide database. Landslide inventory was partitioning using a ratio of the samples in the training and testing datasets of a 70:30 proportion. The results were as following.

- For InSAR components from DEMs SRTM3, SRTM1, and Topo-map, only coherence values had a significant relationship (p-value<0.05) with the events.
- Palsar-RTC data only had a significant effect on the unwrapped phase (p-value=0.02).
- The WofE analysis gave InSAR coherence values between 0.43 and 0.67 with the highest association to landslide events with DEMs SRTM1, SRTM3, and Topo-map.

- Displacement values between 0.14 and 0.19 m from interferograms formed with the DEMs SRTM1 and Topo-map had the highest relationship with landslides. Displacements estimated are in LOS direction.
- The likelihood range obtained with logistic regression posterior-probability of Arc-SDM toolbox was low. Thus, it is necessary to include other variables for building the landslide detection model, i.e., PolSAR and PS-InSAR approach.

Finally, those above was checked with the Tukey test with level confidence of 95%. For InSAR-coherence, all clusters were grouped around 0: meaning no significant differences in coherence for any DEM. However, the opposite was found in the unwrapped phase and displacement varying the DEM, except between SRTM3 and PalsarRTC data.

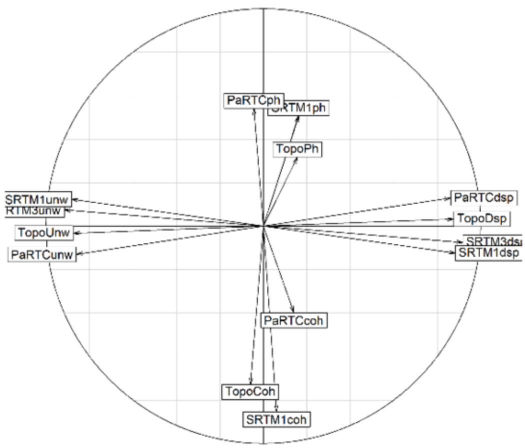

Figure 5. PCA of InSAR components for landslide events.

4. Conclusions

For statistical distribution, InSAR phase has Gaussian behavior, while InSAR coherence and unwrapped phase have a positive skewness with a right tail (high values but low frequency). InSAR displacement showed negative skewness, especially with SRTM3, SRTM1, and Topo-map.

Under the null hypothesis of correlation coefficient equal zero for the independence assumption, the PCA gave that all InSAR components were independent due to the specific location of variables in the correlation circle. However, the correlation between the unwrapped phase and displacement had better representation on the first factorial plane.

This study showed a perfect inverse linear relationship between the unwrapped phase and displacement in the whole experiment using any DEM.

We only had significant InSAR mean differences for unwrapped phase and displacement in LOS direction. These due to spatial resolution and DEMs inaccuracies.

These results ratified the potential of SRTM1-DEM for the processes of co-registration, removing the topographic phase, and geocoding in an InSAR workflow processing, especially for InSAR coherence.

References

[1] C. Colesanti and J. Wasowski, "Investigating landslides with space-borne Synthetic Aperture Radar (SAR) interferometry," *Eng. Geol.*, vol. 88, no. 3–4, pp. 173–199, 2006.
[2] F. Raspini, F. Bardi, S. Bianchini, A. Ciampalini, C. Del Ventisette, P. Farina, F. Ferrigno, L. Solari, and N. Casagli, "The contribution of satellite SAR-derived displacement measurements in landslide risk management practices," *Nat. Hazards*, vol. 86, no. 1, pp. 327–351, 2016.
[3] J. Hu, Z. W. Li, X. L. Ding, J. J. Zhu, L. Zhang, and Q. Sun, "Resolving three-dimensional surface displacements from InSAR measurements: A review," *Earth-Science Rev.*, vol. 133, pp. 1–17, 2014.
[4] F. Rocca and A. Ferretti, "An Overview of SAR Interferometry," pp. 1–13, 2014.
[5] A. Ferretti, A. Monti-Guarnieri, C. Prati, and F. Rocca, *InSAR Principles: Guidelines for SAR Interferometry Processing and Interpretation (TM-19, February 2007)*, no. February. 2007.
[6] W. Teng, L. Mingsheng, and P. Daniel, "InSAR Coherence Decomposition Analysis." pp. 1–5, 2010.
[7] I. Das, S. Sahoo, C. van Westen, A. Stein, and R. Hack, "Landslide susceptibility assessment using logistic regression and its comparison with a rock mass classification system, along a road section in the northern Himalayas (India)," *Geomorphology*, vol. 114, no. 4, pp. 627–637, 2010.
[8] I. Das, A. Stein, N. Kerle, and V. K. Dadhwal, "Landslide susceptibility mapping along road corridors in the Indian Himalayas using Bayesian logistic regression models," *Geomorphology*, vol. 179, pp. 116–125, 2012.
[9] R. N. Afungang, R. Ngoufo, and C. AnguhNkwemoh, "Predicting the Susceptibility of Bamenda Escarpment Zone, NW Cameroon to Landslides Using Logistic Regression Model," *J. Earth Environ. Sci.*, vol. 2017, no. 07, pp. 1–11, 2017.
[10] L. Lombardo and P. M. Mai, "Presenting logistic regression-based landslide susceptibility results," *Eng. Geol.*, vol. 244, no. January, pp. 14–24, 2018.
[11] L. A. Brahim and M. Elmoulat, "Application Of Logistic Regression Method To Produce Landslide Susceptibility Map : A Case Study Of Tetouan Mazari , Morocco," vol. 02082, pp. 1–7, 2018.
[12] F. Bardi, W. Frodella, A. Ciampalini, S. Bianchini, C. Del Ventisette, G. Gigli, R. Fanti, S. Moretti, G. Basile, and N. Casagli, "Integration between ground based and satellite SAR data in landslide mapping: The San Fratello case study," *Geomorphology*, vol. 223, pp. 45–60, 2014.
[13] R. Czikhardt, J. Papco, M. Bakon, P. Liscak, P. Ondrejka, and M. Zlocha, "Ground Stability Monitoring of Undermined and Landslide Prone Areas by Means of Sentinel-1 Multi-Temporal InSAR, Case Study from Slovakia," *Geosciences*, vol. 7, no. 3, p. 87, 2017.
[14] A. Ferretti, A. Monti-Guarnieri, C. Prati, and F. Rocca, "Part B. InSAR processing: a practical approach," 2007.
[15] A.-H. Sultan, "Suitability of DEMs derived from SAR interferometry and ASTER stereoscopy for hydrological applications using GIS," 2009.
[16] R. M. Goldstein and C. L. Werner, "Radar interferogram filtering for geophysical applications," *Geophys. Res. Lett.*, vol. 25, no. 21, pp. 4035–4038, 1998.
[17] C. W. Chen and H. A. Zebker, "Phase unwrapping for large SAR interferograms: Statistical segmentation and generalized network models," *IEEE Trans. Geosci. Remote Sens.,* vol. 40, no. 8, pp. 1709–1719, 2002.
[18] L. D. Kemp, G. F. Bonham-Carter, G. L. Raines, and C. G. Looney, *Arc-SDM: Arcview extension for spatial data modelling using weights of evidence, logistic regression, fuzzy logic and neural network analysis*. São Paulo: Instituto de Geociências, Universidade Estadual de Campinas, 2001.
[19] V. Chaplot, F. Darboux, H. Bourennane, S. Leguédois, N. Silvera, and K. Phachomphon, "Accuracy of interpolation techniques for the derivation of digital elevation models in relation to landform types and data density," *Geomorphology*, vol. 77, no. 1–2, pp. 126–141, 2006.
[20] T. Hengl, *A Practical guide to Geostatistical Mapping*. 2009.
[21] B. Bayer, D. Schmidt, and A. Simoni, "The Influence of External Digital Elevation Models on PS-InSAR and SBAS Results : Implications for the Analysis of Deformation Signals Caused by Slow Moving Landslides in the," *IEEE Trans. Geosci. Remote Sens.*, pp. 1–14, 2017.
[22] R. Mahalingam and M. J. Olsen, "Evaluation of the influence of source and spatial resolution of DEMs on derivative products used in landslide mapping," *Geomatics, Nat. Hazards Risk*, vol. 7, no. 6, pp. 1835–1855, 2016.
[23] J. A. Richards, "Thematic mapping from multitemporal image data using the principal components transformation," *Remote Sensing of Environment*, vol. 16, no. 1. pp. 35–46, 1984.